Electron-Transfer Fluorescence Quenching of Aromatic Hydrocarbons by Europium and Ytterbium Ions in Acetonitrile

Taeko Inada,*,† Yoko Funasaka,† Koichi Kikuchi,† Yasutake Takahashi,‡ and Hiroshi Ikeda§

Department of Physics, School of Science, Kitasato University, 1-15-1 Kitasato, Sagamihara 228-8555, Japan, Department of Materials, Faculty of Engineering, Mie University, Tsu, Mie 514, Japan, and Department of Chemistry, Faculty of Science, Tohoku University, Aoba, Aramaki, Aoba-ku, Sendai 980-8578, Japan

Received: July 21, 2005; In Final Form: December 5, 2005

To make the effects of molecular size on photoinduced electron-transfer (ET) reactions clear, the ET fluorescence quenching of aromatic hydrocarbons by trivalent lanthanide ions M^{3+} (europium ion Eu^{3+} and ytterbium ion Yb^{3+}) and the following ET reactions such as the geminate and free radical recombination were studied in acetonitrile. The rate constant k_q of fluorescence quenching, the yields of free radical (Φ_R) and fluorescer triplet (Φ_T) in fluorescence quenching, and the rate constant k_{rec} of free radical recombination were measured. Upon analysis of the free energy dependence of k_q, Φ_R, Φ_T, and k_{rec}, it was found that the switchover of the fluorescence quenching mechanism occurs at $\Delta G_{fet} = -1.4$ to -1.6 eV: When $\Delta G_{fet} < -1.6$ eV, the fluorescence quenching by M^{3+} is induced by a long-distance ET yielding the geminate radical ion pairs. When $\Delta G_{fet} > -1.4$ eV, it is induced by an exciplex formation. The exciplex dissociates rapidly to yield either the fluorescer triplet or the geminate radical ion pairs. The large shift of switchover ΔG_{fet} from -0.5 eV for aromatic quenchers to -1.4 to -1.6 eV for lanthanide ions is almost attributed to the difference in the molecular size of the quenchers. Furthermore, it was substantiated that the free energy dependence of ET rates for the geminate and free radical recombination is satisfactorily interpreted within the limits of the Marcus theory.

1. Introduction

The electron-transfer (ET) process is one of the most important phenomena in chemistry and biology. Therefore, a large number of investigations on ET fluorescence quenching have been carried out to clear how the ET rate can be controlled. The ET reaction is well-known to depend on various factors such as the free energy change (ΔG_{et}) of full ET, the solvent polarity, the reaction distance, the molecular properties of the electron donor and acceptor (EDA), and so on.

In previous work,[1] a detailed mechanism of ET fluorescence quenching has been investigated in polar solvents such as acetonitrile, methanol, and 1,2-dichloromethane using aromatic compounds as fluorescers and quenchers. It was established that the ET fluorescence quenching mechanism depends on the free energy change (ΔG_{fet}) of full ET in fluorescence quenching. In polar solvents, the switchover of the fluorescence quenching mechanism occurs at $\Delta G_{fet} \approx -0.5$ eV. When $\Delta G_{fet} > -0.5$ eV, the fluorescence quenching is induced by an exciplex formation (or a partial ET followed by radiative and nonradiative processes). When $\Delta G_{fet} < -0.5$ eV, the fluorescence quenching is induced by a long-distance ET (or a full ET followed by free radical generation and geminate radical recombination). It is noted that ΔG_{fet} and the free energy change (ΔG_{bet}) of back ET within the geminate radical ion pairs (GRIPs) in the electronically ground state and also encounter free radical ion pairs were evaluated as follows[2]

$$\Delta G_{fet} = E_{1/2}^{ox} - E_{1/2}^{red} + z_D z_A e^2/\epsilon r_q - E(S_1) \quad (1)$$

$$\Delta G_{bet} = E_{1/2}^{red} - E_{1/2}^{ox} - z_D z_A e^2/\epsilon r_{bet} \quad (2)$$

Here, $E_{1/2}^{ox}$, $E_{1/2}^{red}$, and $E(S_1)$ are the oxidation potential of the electron donor, the reduction potential of the electron acceptor, and the energy of the fluorescent state. z_D and z_A are the charges of the electron donor and acceptor, respectively. The subscripts D and A stand for the electron donor and acceptor in fluorescence quenching. ϵ is the dielectric constant of the solvent. r_q and r_{bet} are the center-to-center separation of the electron acceptor and donor at the instant of fluorescence quenching and back ET, respectively.

When molecular oxygen (O_2) and thiocyanate ion (SCN^-) were used as the quenchers for the fluorescence quenching of aromatic compounds in acetonitrile, the quenching mechanism was found to be predominantly the short-lived exciplex formation and the free radical generation was observed only in the case of SCN^- at a highly exothermic region, that is, $\Delta G_{fet} < -1.0$ eV.[3b,4] These results indicate that the switchover ΔG_{fet} for SCN^- and O_2 shifts to the more negative region than -1.0 eV. Such a large shift of the switchover ΔG_{fet} from -0.5 eV for aromatic quenchers to -1.0 eV for SCN^- and O_2 has accounted for the difference in the molecular size of quenchers. According to the Marcus theory,[5] the solvent reorganization energy λ_s increases with decreasing molecular size and the increase of λ_s decreases the rate of long-distance ET in the normal region. In the study of the ΔG_{fet} dependence of the ET

* To whom correspondence should be addressed. E-mail: tinada@jet.sci.kitasato-u.ac.jp.
† Kitasato University.
‡ Mie University.
§ Tohoku University.

10.1021/jp054027m CCC: $33.50
Published on Web 02/03/2006

fluorescence quenching mechanism by use of various kinds of quenchers, therefore, it is necessary to make the size of the quenchers even. According to this point of view, several studies on the ET fluorescence quenching by inorganic ions may be reviewed as follows.

As for metal ion quenchers, Sabbatini et al.[6] carried out a systematic study on the fluorescence and triplet quenching in acetonitrile using the europium ion as a quencher and found that (i) the fluorescence quenching takes place at a diffusion-controlled limit in the region $-2.6 < \Delta G_{fet} < -1.3$ eV, (ii) the radical cations of fluorescers are generated with high efficiencies in the fluorescence quenching of anthracene with $\Delta G_{fet} - z_D z_A e^2/\epsilon r_q = -2.34$ eV and tetracene with $\Delta G_{fet} - z_D z_A e^2/\epsilon r_q = -1.98$ eV, and (iii) the triplet quenching takes place at a very low rate ($\approx 10^6$ M^{-1} s^{-1}) in the region $-1.3 < \Delta G_{fet} - z_D z_A e^2/\epsilon r_q < -0.4$ eV. The findings (i) and (ii) seem to indicate that the fluorescence quenching mechanism in the region $-2.6 < \Delta G_{fet} - z_D z_A e^2/\epsilon r_q < -1.3$ eV is a long-distance ET. However, the high efficiency of enhanced intersystem crossing in the fluorescence quenching of coronene with $\Delta G_{fet} - z_D z_A e^2/\epsilon r_q = -1.87$ eV suggests that the fluorescence quenching is due to an exciplex formation. These contradictory results require further experiments on the fluorescence quenching in the region not only $-2.6 < \Delta G_{fet} - z_D z_A e^2/\epsilon r_q < -1.3$ eV but also $\Delta G_{fet} - z_D z_A e^2/\epsilon r_q > -1.3$ eV. Unfortunately, the finding (iii) on the triplet quenching in the region $\Delta G_{fet} - z_D z_A e^2/\epsilon r_q > -1.3$ eV gives no information on the fluorescence quenching mechanism owing to the extremely different aspects of fluorescence and triplet quenching.

As for halogen anion quenchers, Shizuka et al.[7] carried out a systematic study on the fluorescence quenching by I^- and Br^- in a water−ethanol 1:1 mixed solvent. The quenching takes place at the diffusion-controlled limit in the region -0.78 eV $< \Delta G_{fet} < -0.2$ eV, yielding no transient species due to full ET. In the region $\Delta G_{fet} > -0.2$ eV, the quenching rate decreases with increasing ΔG_{fet} in a moderate way compared with the Rehm−Weller plot. The participation of an enhanced intersystem crossing with high efficiency in the fluorescence quenching was confirmed for fluorescers such as anthracene (with $\Delta G_{fet} = -0.2$ eV for I^- and -0.40 eV for Br^-) and phenanthrene (with $\Delta G_{fet} = -0.04$ eV for I^- and -0.64 eV for Br^-). These results indicate that the fluorescence quenching is induced by a contact collision of the fluorescer with a halogen anion giving rise to a short-lived charge-transfer complex (or an exciplex) where the enhanced intersystem crossing takes place rapidly.[8]

Recently, the formation of free radicals in the fluorescence quenching by a halogen anion has been reported for the 1-cyanonaphthalene−I^- pair with $\Delta G_{fet} = -1.0$ eV and the 9,10-dicyanoanthracene−I^- pair with $\Delta G_{fet} = -1.09$ eV at such a high iodine concentration as 0.03 M in acetonitrile.[9] However, it has not been determined whether the fluorescence quenching mechanism is a long-distance ET or an exciplex formation.

In this work, we establish the fluorescence quenching mechanism of aromatic hydrocarbons by trivalent lanthanide ions M^{3+} (i.e., the europium ion Eu^{3+} and ytterbium ion Yb^{3+}) in acetonitrile. On the basis of a comprehensive study involving (1) the ΔG_{fet} dependence of k_q over a wide range of ΔG_{fet} from 0.01 to -2.02 eV, (2) the ΔG_{bet} dependence of the rate of back ET within GRIP (k_{bet}), (3) the ΔG_{bet} dependence of the rate of free radical recombination (k_{rec}), and (4) the ΔG_{fet} dependence of the triplet yield in fluorescence quenching, it is shown that the switchover of the fluorescence quenching mechanism occurs around $\Delta G_{fet} = -1.5$ eV. The fluorescence quenching is induced by a long-distance ET in the region $\Delta G_{fet} < -1.5$ eV and by an instantaneous exciplex formation in the region $\Delta G_{fet} > -1.5$ eV. Furthermore, it is shown that the ΔG_{bet} dependence of either k_{bet} or k_{rec} is well reproduced by the semiclassical equation for long-distance ET[10−12] with the same fitting parameters as those used in previous work on aromatic quenchers other than the parameter of quencher size.

2. Experimental Section

The methods for synthesis and/or purification of 9-cyanoanthracene (CA), 9-phenylanthracene (PA), 9,10-dicyanoanthracene (DCA), 1,2,9,10-tetracyanoanthracene (1,2,9,10-TeCA), 2,6,9,10-tetracyanoanthracene (2,6,9,10-TeCA), perylene (Per), anthracene (An), 9,10-diphenylanthracene (DPAn), 1,2-benzanthracene (BAn), benzo[*ghi*]perylene (BPer), and fluoranthene (Flu) have been reported elsewhere.[1c,g,h] Rubrene (Rub) was purified using thin-layer chromatography. Europium perchlorate (Soekawa), ytterbium perchlorate (Soekawa), and acetonitrile (SP grade, Kanto) were used as received.

Absorption spectra were recorded on a Hitachi U-3500 spectrophotometer. Fluorescence spectra and fluorescence excitation spectra were measured with a Hitachi F-4500 spectrophotometer. The fluorescence lifetimes (τ_F^0) were measured with a Horiba NAES-700 fluorometer. τ_F^0 values in acetonitrile are 15.9 ns for 1,2,9,10-TeCA, 17.7 ns for 2,6,9,10-TeCA, 16.5 ns for DCA, 17.1 ns for CA, 16.5 ns for Rub, 5.5 ns for Per, 8.7 ns for DPAn, 42.1 ns for BAn, 127 ns for BPer, 46.0 ns for Flu, and 4.9 ns for An. The transient absorption spectra were measured by conventional microsecond flash photolysis. The free radical yield Φ_R and the triplet yield Φ_T in fluorescence quenching were determined by an emission−absorption flash photolysis method.[1,13] This method measures the fluorescence intensity during a flash excitation and the initial absorbance of transient absorption simultaneously. The former is used to evaluate the amount of light absorbed by a sample solution, and the latter is used to determine the concentration of transient species produced by a flash excitation. Error limits of this method for determining Φ_R and Φ_T are within 10%. The photophysical parameters necessary to determine Φ_R and Φ_T have been reported elsewhere[1d,3b] except for anthracene and Rub. The molar extinction coefficients of transient absorption due to the anthracene triplet and anthracene radical cation were determined to be 73 100 M^{-1} cm^{-1} at 420 nm and 11 700 M^{-1} cm^{-1} at 715 nm in acetonitrile, respectively. The quantum yield of intersystem crossing was determined to be 0.68 in acetonitrile.[14] The rate constant k_{rec} of free radical recombination was determined from the decay curve of the transient absorption due to the free radial cations ($F^{\bullet +}$) of fluorescers assuming that they recombine with the counter radical cations ($M^{\bullet 2+}$) of quenchers. The reduction potentials $E_{1/2}^{red}$ vs the saturated calomel electrode (SCE) were measured in acetonitrile with 0.1 M tetraethylammonium perchlorate as the supporting electrolyte: -0.09 V for Eu^{3+} and -0.86 V for Yb^{3+}. The $E_{1/2}^{ox}$ values for fluorescers in acetonitrile have been reported as follows: 1.47 V for Rub, 1.57 V for CA, 1.89 V for DCA, 2.20 V for 1,2,9,10-TeCA, 2.11 V for 2,6,9,10-TeCA, 0.98 V for Per, 1.09 V for An, 1.19 V for DPAn, 1.31 V for BAn, 1.03 V for BPer, and 1.65 V for Flu.[1,3b,15] All measurements were made at 298 K.

3. Results and Discussion

3.1. Fluorescence Quenching. The rate constants k_q of fluorescence quenching by M^{3+} were determined from the Stern−Volmer plots for the fluorescence intensity at low quencher concentration (<10 mM), where the plots were linear. Under this condition, the EDA complex formation was not

TABLE 1: Free Energy Changes of ET Fluorescence Quenching (ΔG_{fet}), Fluorescence Quenching Rate Constants (k_q), and Effective Quenching Distances (r_q)

fluorescer	quencher	ΔG_{fet} (eV)	k_q (10^{10} M^{-1} s^{-1})	r_q [a] (Å)
1,2,9,10-TeCA	Eu^{3+}	−0.21[b]	0.027	
2,6,9,10-TeCA	Eu^{3+}	−0.45[b]	0.22	
CA	Yb^{3+}	−0.47[b]	0.24	
Rub	Yb^{3+}	−0.59	0.40	5.0
DCA	Eu^{3+}	−0.79	0.42	5.5
Per	Yb^{3+}	−0.89	0.50	6.6
DPAn	Yb^{3+}	−0.93	0.48	6.3
BAn	Yb^{3+}	−0.94	0.48	6.3
BPer	Yb^{3+}	−1.10	0.55	7.3
Flu	Eu^{3+}	−1.21	0.53	7.0
An	Yb^{3+}	−1.22	0.52	6.8
CA	Eu^{3+}	−1.28	0.58	7.0
Rub	Eu^{3+}	−1.38	0.53	8.0
Per	Eu^{3+}	−1.69	0.60	7.9
DPAn	Eu^{3+}	−1.72	0.60	7.9
BAn	Eu^{3+}	−1.74	0.68	8.9
BPer	Eu^{3+}	−1.89	0.67	8.8
An	Eu^{3+}	−2.02	0.70	9.3

[a] The values of r_q except for Rub were evaluated from k_q by the use of eq 3. [b] Calculated by assuming $r_q = 5.0$ Å.

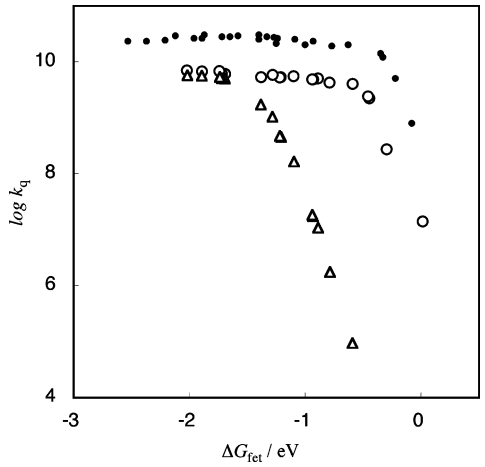

Figure 1. Plots of k_q vs ΔG_{fet}: experimental (○) and theoretical plots (Δ) for trivalent lanthanide ions and experimental plot (●) for aromatic quenchers. The theoretical plot was calculated by eq 12 with r_q listed in Table 1 and the fitting parameters used to draw the theoretical curve shown in Figure 3.

detected by absorption spectroscopy. The values for k_q and ΔG_{fet} are listed in Table 1. The plot of log k_q vs ΔG_{fet} is shown in Figure 1 (○).

This plot is somewhat different from the plot obtained for aromatic quenchers (●)[1f,g]: The k_q values for lanthanide ions are about four times smaller than those for aromatic quenchers throughout ΔG_{fet}. In the region $\Delta G_{fet} < -0.5$ eV, the k_q value for lanthanide ions slightly increases with decreasing ΔG_{fet} in a similar way as that for aromatic quenchers. Such ΔG_{fet} dependence of k_q is one of characteristics for the diffusion-controlled ET fluorescence quenching. Therefore, the fluorescence quenching by lanthanide ions is considered to take place at the diffusion-controlled limit (k_{dif}) in the region $\Delta G_{fet} < -0.5$ eV.

The effective quenching distance r_q was measured by use of the modified Stern−Volmer equation[16] at such high quencher concentration as >0.1 M. At such a high concentration of Eu^{3+} and Yb^{3+}, the measurement for determining r_q was possible only when Rub was used as a fluorescer, because the absorption spectra of fluorescers other than Rub overlapped with those of

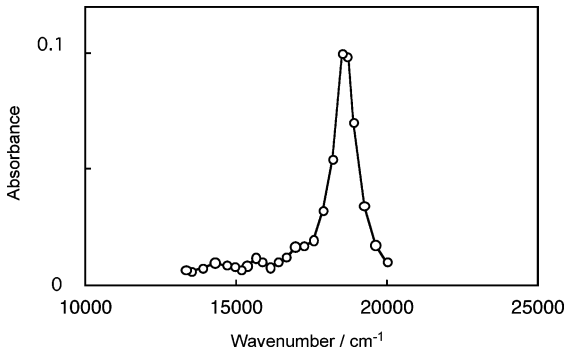

Figure 2. Transient spectrum observed for the Per−Eu^{3+} pair.

Eu^{3+} and Yb^{3+}. The r_q values were determined to be 5.0 and 8.0 Å for Yb^{3+} and Eu^{3+}, respectively.

When the quenching takes place at the diffusion-controlled limit, k_q is related to r_q as follows[16,17]

$$k_{dif} = k_q = 4\pi r_q D N_A \tag{3}$$

Here, D (in units of cm^2 s^{-1}) is the sum of the diffusion coefficients of two particles in solution and N_A is Avogadro's number. In the cases of the Rub−Eu^{3+} and Rub−Yb^{3+} pairs, $k_q = 5.3 \times 10^9$ and 4.0×10^9 M^{-1} s^{-1} and $r_q = 8.0$ and 5.0 Å, respectively. Putting these values into eq 3, we obtain $D = 8.7 \times 10^{-6}$ cm^2 s^{-1} for Rub−Eu^{3+} and 1.1×10^{-5} cm^2 s^{-1} for Rub−Yb^{3+}. As the difference in D between two kinds of EDA pairs is small, it is assumed, hereafter, that the average value $D = 1.0 \times 10^{-5}$ cm^2 s^{-1} can be applied to all the EDA pairs listed in Table 1. Then, it is possible to evaluate r_q from k_q by use of eq 3 as listed in Table 1. It is noted that the r_q values listed in Table 1 were used to calculate ΔG_{fet}.

Flashing of the solution containing a fluorescer (10^{-4}−10^{-5} M) and a lanthanide ion (1−5 mM) gave the transient absorption due to fluorescer radical cations, when Rub, Per, DPAn, BAn, BPer, Flu, and An were used as the fluorescers. Figure 2 shows the transient absorption spectrum for the Per−Eu^{3+} pair.

When anthracenecarbonitriles were used as the fluorescers, no transient absorption was observed. When Yb^{3+} was used as the quencher, the enhanced intersystem crossing due to fluorescence quenching was observed for Rub, Per, DPAn, BAn, and An. This is due to the fact that the triplet energies $E(T_1)$ of fluorescers are smaller than the energies ($-\Delta G_{bet}$) of the corresponding GRIP. The free radical yields (Φ_R) and the triplet yields (Φ_T) in fluorescence quenching were determined as listed in Table 2. Φ_R increases with increasing ΔG_{bet} in the region $-2.3 < \Delta G_{bet} < -1.1$ eV.

3.2. Back Electron Transfer within GRIP. If the fluorescence quenching is induced by the long-distance ET for producing GRIP as shown in Scheme 1, the efficiency of GRIP production in fluorescence quenching is unity.

SCHEME 1

$$^1F^* + M^{3+} \underset{k_{-dif}}{\overset{k_{dif}}{\rightleftharpoons}} (^1F^*/M^{3+}) \xrightarrow[\Delta G_{fet}]{k_{fet}} \overset{\text{GRIP}}{(F^{\bullet+}/M^{\bullet 2+})} \xrightarrow{k_{esc}} F^{\bullet+}.....M^{\bullet 2+}$$
$$(F^{\bullet+}/M^{\bullet 2+}) \xrightarrow{k_{bet}} F + M^{3+}$$

Here, the parentheses indicate the encounter state. Then, Φ_R is given by eq 4

$$\Phi_R = k_{esc}/(k_{esc} + k_{bet}) \tag{4}$$

Here, k_{esc} is the rate constant for GRIP separation into free

TABLE 2: Free Energy Changes of ET Fluorescence Quenching (ΔG_{fet}) and of the Back ET within GRIP (ΔG_{bet}), Free Radical Yields (Φ_R), and Triplet Yields (Φ_T) in Fluorescence Quenching, Rate Constants of GRIP Separation into Free Radicals (k_{esc}), Back ET within GRIP (k_{bet}), Free Radical Recombination (k_{rec}), and Energies of the Lowest Triplet ($E(T_1)$)

fluorescer	quencher	ΔG_{fet} eV	Φ_R	Φ_T	k_{esc} 10^9 s^{-1}	k_{bet} 10^9 s^{-1}	k_{rec} 10^9 M^{-1} s^{-1}	ΔG_{bet} eV	$E(T_1)$ eV
Per	Yb^{3+}	−0.89	0.14	0.044	10.1	62.0[a] (65.4)[b]	1.04	−1.96	1.60
DPAn	Yb^{3+}	−0.93	0.096	0.024	11.6	109[a] (112)[b]	0.98	−2.17	1.73
BAn	Yb^{3+}	−0.94	0.067	0.10	11.6	161[a] (180)[b]	1.26	−2.29	2.05
BPer	Yb^{3+}	−1.10	0.14	0.008	7.55	46.4[a] (46.8)[b]	1.06	−2.00	2.01
Flu	Eu^{3+}	−1.21	0.19	0	8.54	36.4[a]	[c]	−1.85	2.29
An	Yb^{3+}	−1.22	0.072	0.11	9.29	120[a] (135)[b]	1.06	−2.06	1.74
Per	Eu^{3+}	−1.69	0.92	0	6.00	0.52[a]	0.077	−1.17	1.60
DPAn	Eu^{3+}	−1.72	0.67	0	6.00	2.96[a]	0.27	−1.38	1.73
BAn	Eu^{3+}	−1.74	0.45	0	4.25	5.20[a]	0.67	−1.49	2.05
An	Eu^{3+}	−2.02	0.82	0	3.75	0.82[a]	0.13	−1.26	1.74

[a] k_{bet} was evaluated from Φ_R by the use of eq 4. [b] k_{bet} was evaluated from Φ_R and Φ_T by the use of eqs 14 and 15. [c] The decay of $Flu^{\bullet+}$ was not second order.

radicals. According to the Tachiya theory,[18] k_{esc} is given by eq 5

$$k_{esc} = Dr_c/[r_q^3\{1 - \exp(-r_c/r_q)\}] \quad (5)$$

Here, r_c is the Onsager distance

$$r_c = z_D z_A e^2/\epsilon k_B T \quad (6)$$

Here, k_B is the Boltzman constant. Putting $z_D = +1$ and $z_A = +2$, we obtain $r_c = 28.8$ Å.

If the fluorescence quenching mechanism is the long-distance ET for producing GRIP, the rate constant (k_{bet}) of back ET within GRIP evaluated by use of eq 4 may fit in with the semiclassical theory of long-distance ET.[10−12] However, it is not clear whether the fluorescence quenching with lanthanide ions is induced by the long-distance ET. Therefore, we temporarily use eq 4 to evaluate k_{bet} for all the EDA pairs for which the Φ_R values have been determined. The k_{bet} values thus evaluated are used to decide the quenching mechanism for each EDA pair. The values for ΔG_{bet}, Φ_R, k_{esc}, and k_{bet} are summarized in Table 1. Figure 3 (●) shows the plot of k_{bet} vs ΔG_{bet}.

When the back ET within GRIP takes place at the distance r_{bet}, the rate of back ET may be given by the following semiclassical equation for long-distance ET[10−12]

$$k_{et} = (4\pi^3/h^2\lambda_S k_B T)^{1/2}|V|^2 \Sigma\,(e^{-S}S^w/w!)\exp[-(\Delta G_{et} + \lambda_S + whv)^2/4\lambda_S k_B T] \quad (7)$$

Here

$$\lambda_S = e^2(1/2r_A + 1/2r_D - 1/r_{et})(1/n^2 - 1/\epsilon) \quad (8)$$

$$|V|^2 = |V_0|^2 \exp[-\beta\{r_{et} - (r_A + r_D)\}] \quad (9)$$

$$S = \lambda_v/hv$$

r_D and r_A are the radii of electron donor and acceptor, r_{et} is their center-to-center separation at the instant of ET, and n is the solvent refractive index. It is noted that $k_{et} = k_{fet}$ and $r_{et} = r_q$ for the case of ET fluorescence quenching and $k_{et} = k_{bet}$ and $r_{et} = r_{bet}$ for the cases of the back ET within the GRIP and the encountered free radical pairs.

To fit the theory and experiment as best we can, the parameters other than r_{et} and the radii for M^{3+} and M^{2+} were assumed to be the same as those used in the previous work on the aromatic fluorescer and quencher pairs in acetonitrile:[1e−g]

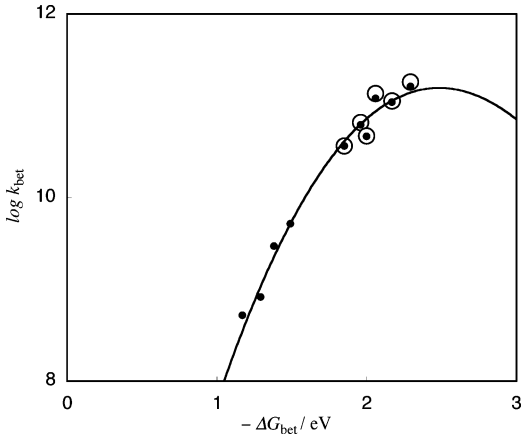

Figure 3. Plots for k_{bet} vs ΔG_{bet}: the k_{bet} values are evaluated by eq 4 (○) and by eqs 14 and 15 (●). The solid curve was calculated by eq 7 with fitting parameters $\beta = 1.0$ Å^{-1}, $\lambda_v = 0.25$ eV, $r_D = 3$ Å, $r_A = 1.9$ Å, $h\nu = 1500$ cm^{-1}, $|V_0| = 120$ cm^{-1}, $r_{bet} = 7.5$ Å, and $\lambda_s = 2.26$ eV.

the reactant vibrational reorganization energy, $\lambda_v = 0.25$ eV; the average energy of active vibrational mode, $h\nu = 1500$ cm^{-1}; the radii of aromatic molecules, 3 Å; the attenuation parameter, $\beta = 1$ Å^{-1}; the electron exchange matrix element at contact distance of the EDA pair, $|V_0| = 120$ cm^{-1}. The best fitting curve for the plot of k_{bet} vs ΔG_{bet} was obtained by setting $r_A = 1.9$ Å, $r_{bet} = 7.5$ Å, and $\lambda_s = 2.26$ eV as shown in Figure 3. In the case of the aromatic fluorescer and quencher pairs, the best fitting curve was obtained by setting $r_A = 3.0$ Å, $r_{bet} = 7.5$ Å, and $\lambda_s = 1.52$ eV. The increase in λ_s from 1.52 eV for aromatic quenchers to 2.26 eV for lanthanide ions is due to the decrease in r_A from 3.0 to 1.9 Å. Therefore, a remarkable difference in the ΔG_{bet} dependence of k_{bet} between aromatic quenchers and lanthanide ions is attributed to the difference in the radii of the quenchers. It is noteworthy that the sum of $r_D = 3.0$ Å and $r_A = 1.9$ Å is close to the effective quenching distance 5.0 Å for the Rub−Yb^{3+} pair.

3.3. Free Radical Recombination. The rate constants k_{rec} of free radical recombination have been determined as listed in Table 2 and are plotted with respect to ΔG_{bet} in Figure 4 (○). k_{rec} increases with decreasing ΔG_{bet} in the region $\Delta G_{bet} > -2.0$ eV and is almost constant in the region $\Delta G_{bet} < -2.0$ eV. The mechanism of free radical recombination can be described as Scheme 2.

SCHEME 2

$$F^{\bullet+} + M^{\bullet 2+} \underset{k_{-dif}}{\overset{k_{dif}}{\rightleftharpoons}} (F^{\bullet+}/M^{\bullet 2+}) \xrightarrow{k_{bet}} (F + M^{3+})$$

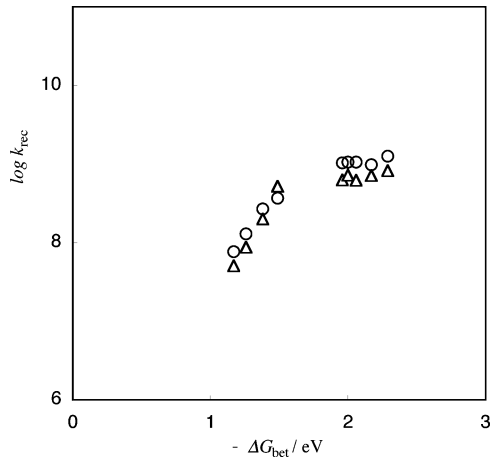

Figure 4. Plots for k_{rec} vs ΔG_{bet}: experimental (○) and theoretical plots (Δ). The theoretical plot was calculated by eqs 5, 7, and 11 with the fitting parameters other than r_{bet} used to draw the theoretical curve shown in Figure 3. Here, the following r_{bet} values were used for eqs 5, 7, and 11: 7 Å for the Per−Eu^{3+} pair, 7.5 Å for the DPAn−Eu^{3+} and An−Eu^{3+}pairs, 8 Å for the BAn−Eu^{3+} pair, 9 Å for the BPer−Yb^{3+}, An−Yb^{3+}, and Per−Yb^{3+}pairs, and 10 Å for the BAn−Yb^{3+} and DPAn−Yb^{3+} pairs.

According to Scheme 2, k_{rec} may be described as follows

$$k_{rec} = k_{dif}k_{bet}/(k_{-dif} + k_{bet}) \quad (10)$$

Here, k_{dif} is given by eq 11[19]

$$k_{dif} = 4\pi DN_A r_c/\{\exp(r_c/r_{bet}) - 1\} \quad (11)$$

k_{-dif} is given by eq 5, and k_{bet} may be given by eqs 7−9 with the parameters used to obtain the theoretical curve shown in Figure 3. To evaluate the k_{rec} according to eq 10, we assume that the ΔG_{bet} dependence of r_{bet} in eq 11 is the same as the ΔG_{fet} dependence of r_q.

As shown in Figure 4, the theoretical plots (Δ) almost fit in with the experimental plots (○). Therefore, the free radical recombination is caused by a long-distance ET as expected.

3.4. ET Fluorescence Quenching Mechanism. Applying the steady state approximation to Scheme 1, we obtain eq 12.

$$k_q = k_{dif}k_{fet}/(k_{fet} + k_{-dif}) \quad (12)$$

The rate (k_{fet}) of fluorescence quenching due to a long-distance ET from aromatic hydrocarbons to lanthanide ions can be calculated by the use of eq 7 together with the fitting parameters given in section 3.2. If there is no Coulombic interaction between the fluorescer and the quencher, k_{-dif} may be given by eq 13[18]

$$k_{-dif} = D/r_q^2 \quad (13)$$

The k_q values calculated by the use of eqs 3, 12, and 13 are plotted with respect to ΔG_{fet} as shown in Figure 1 (Δ). This theoretical plot (Δ) agrees with the experimental plot (○) in the region $\Delta G_{fet} < -1.6$ eV but does not agree in the region $\Delta G_{fet} > -1.4$ eV. In contrast, this theoretical plot is consistent with the plot of k_{rec} vs ΔG_{bet} shown in Figure 4, because the disagreement of these plots is not due to k_{et} itself but to the difference in the Coulombic interaction between two kinds of encounter pairs, that is, ($^1F^*/M^{3+}$) and ($F^{\bullet+}/M^{\bullet 2+}$): The k_{dif} and k_{-dif} for ($^1F^*/M^{3+}$) with $r_q = 7.5$ Å are calculated, respectively, to be 5.7×10^9 s^{-1} and 1.8×10^9 s^{-1} by the use of eqs 3 and 13, and the k_{dif} and k_{-dif} for ($F^{\bullet+}/M^{\bullet 2+}$) with $r_{bet} = 7.5$ Å are calculated, respectively, to be 4.3×10^8 and 1.1×10^{10} s^{-1} by the use of eqs 11 and 5. The exciplex formation does not participate in the free radical recombination but does in the fluorescence quenching. Therefore, it may be concluded by comparing the theoretical plot (Δ) with the experimental plot (○) in Figure 1 that (i) the fluorescence quenching is induced by the long-distance ET for producing GRIP in the region $\Delta G_{fet} < -1.6$ eV and (ii) by the exciplex formation in the region $\Delta G_{fet} > -1.4$ eV. In the case of the Rub−Yb^{3+} pair with $\Delta G_{fet} = -0.59$ eV, the dominant quenching mechanism is considered to be the exciplex formation judging from a large discrepancy in k_q between the experimental and theoretical plots. As the quenching takes place at the diffusion-controlled limit, the electronic interaction between Rub and Yb^{3+} within the exciplex has to be strong enough to allow a rapid deactivation of the exciplex. Therefore, the quenching distance $r_q = 5.0$ Å for the Rub−Yb^{3+} pair may be regarded as the center-to-center distance of the exciplex. The radii for aromatic molecules are usually assumed to be about 3.0 Å. Then, the radius for Yb^{3+} is estimated to be 2.0 Å, which is consistent with the radius assumed for lanthanide ions in section 3.2, that is, $r_A = 1.9$ Å. In the case of aromatic quenchers, both k_q and r_q decrease with increasing ΔG_{fet} in the downhill region ($-0.5 < \Delta G_{fet} < 0$ eV), where the quenching is induced by an exciplex formation. This is the same even in the case of lanthanide ions, although the corresponding ΔG_{fet} region is expanded to $-1.4 < \Delta G_{fet} < 0$ eV. Moreover, the observation of enhanced intersystem crossing ($\Phi_T > 0$) in the region $-1.3 < \Delta G_{fet} < -0.8$ eV supports the fluorescence quenching due to exciplex formation. The large shift of the switchover ΔG_{fet} from −0.5 eV for aromatic quenchers to −1.4 to −1.6 eV for lanthanide ions is almost attributed to the increase in λ_s : $\lambda_s = 2.26$ eV for lanthanide ions and 1.52 eV for aromatic quenchers.

If the fluorescence quenching is induced by an exciplex formation, then the evaluation of k_{bet} by the use of eq 4 defined according to Scheme 1 is not valid, and hence, the k_{bet} values thus evaluated in the region -1.5 eV $< \Delta G_{fet} < -0.9$ eV (or -2.3 eV $< \Delta G_{bet} < -1.9$ eV) are meaningless. Nevertheless, these k_{bet} values agree with the theoretical curve shown in Figure 3. This fact may indicate the instantaneous exciplex formation followed by its rapid dissociation giving rise to the GRIP and fluorescer triplet.[6−9] The Coulombic repulsion between the exciplex component pair may be responsible for such characteristics of exciplex. In this case, the fluorescence quenching mechanism can be described by Scheme 3, which is considered to be applicable for the region -1.5 eV $< \Delta G_{fet} < 0$ eV.

SCHEME 3

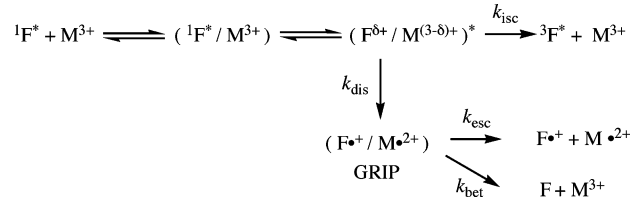

Here, ($^1F^*/M^{3+}$) is the encounter pair and ($^1F^{\delta}+/M^{(3-\delta+)}$)* is the exciplex.

According to Scheme 3, we obtain

$$\Phi_R = \{k_{dif}/(k_{dis} + k_{isc})\}\{k_{esc}/(k_{esc} + k_{bet})\} \quad (14)$$

$$\Phi_T = k_{isc}/(k_{dis} + k_{isc}) \quad (15)$$

The k_{bet} values calculated by the use of eqs 14 and 15 in addition to eq 5 are plotted with respect to ΔG_{bet} as shown in

Figure 3 (○). The k_{bet} thus calculated agrees with the theoretical curve, indicating the validity of Scheme 3 in the region -1.5 eV $< \Delta G_{fet} < -0.9$ eV.

4. Conclusion

In the case of the ET fluorescence quenching by lanthanide ions, the switchover of the fluorescence quenching mechanism occurs at $\Delta G_{fet} = -1.4$ to -1.6 eV. The fluorescence quenching is induced by a long-distance ET in the region $\Delta G_{fet} < -1.6$ eV and by an instantaneous exciplex formation in the region $\Delta G_{fet} > -1.4$ eV. The large shift of the switchover ΔG_{fet} from -0.5 eV for aromatic quenchers to around -1.5 eV for lanthanide ions is almost attributed to the increase in λ_s due to a decrease in the molecular size of the quenchers. The exciplex formation does not reduce in effect the free radical yield owing to the rapid dissociation of the exciplex into the GRIPs. The ΔG_{bet} dependence of k_{rec} is almost interpreted within the frameworks of Marcus theory.

Acknowledgment. We are greatly indebted to Drs. M. Tachiya and S. Murata (National Institute of Advanced Industrial Science and Technology) for their helpful discussions. We are grateful to Dr. H. Matsuzawa (School of Science, Kitasato University) for his advice on the measurement of fluorescence lifetime. We greatly appreciate the referees' valuable comments. The present work is partly defrayed by the Grant-in-Aid for Scientific Research from the Ministry of Education, Science, Sports, and Culture of Japan (16550020). H.I. gratefully acknowledges financial support from a Grant-in-Aid for Scientific Research on Priority Areas (No. 417) from the Ministry of Education, Culture, Sports, Science, and Technology of Japan (No. 14050008), the Izumi Science and Technology Foundation, and the Shorai Foundation.

References and Notes

(1) (a) Kikuchi, K.; Niwa, T.; Takahashi, Y.; Ikeda, H.; Miyashi, T.; Hoshi, M. *Chem. Phys. Lett.* **1990**, *173*, 421−424. (b) Kikuchi, K.; Hoshi, M.; Niwa, T.; Takahashi, Y.; Miyashi, T. *J. Phys. Chem*. **1991**, *95*, 38−42. (c) Kikuchi, K.; Katagiri, T.; Niwa, T.; Takahashi, Y.; Suzuki, T.; Ikeda, H.; Miyashi, T. *Chem. Phys. Lett.* **1992**, *193*, 155−160. (d) Kikuchi, K.; Niwa, T.; Takahashi, Y.; Ikeda, H.; Miyashi, T. *J. Phys. Chem.* **1993**, *97*, 5070−5073. (e) Niwa, T.; Kikuchi, K.; Matsushita, N.; Hayashi, M.; Takahashi, Y.; Miyashi, T. *J. Phys. Chem*. **1993**, *97*, 11960−11964. (f) Niwa, T.; Miyazawa, C.; Kikuchi, K.; Yamauchi, M.; Nagata, T.; Takahashi, Y.; Ikeda, H.; Miyashi, T. *J. Am. Chem. Soc*. **1999**, *121*, 7211−7219. (g) Inada, T.; Kikuchi, K.; Takahashi, Y.; Ikeda, H.; Miyashi, T. *J. Phys. Chem*. A **2002**, *106*, 4345−4349.

(2) Rehm, D.; Weller, A. *Isr. J. Chem*. **1970**, *8*, 259−271.

(3) (a) Kikuchi, K.; Sato, C.; Watabe, M.; Ikeda, H.; Takahashi, Y.; Miyashi, T. *J. Am. Chem. Soc*. **1993**, *115*, 5180−5184. (b) Sato, C.; Kikuchi, K.; Okamura, K.; Takahashi, Y.; Miyashi, T. *J. Phys. Chem.* **1995**, *99* 16925−13931.

(4) Sato, C.; Kikuchi, K.; Ishikawa, H.; Iwahashi, M.; Ikeda, H.; Takahashi, Y.; Miyashi, T. *Chem. Phys. Lett.* **1997**, *276*, 210−216.

(5) (a) Marcus, R. A. *J. Chem. Phys*. **1956**, *24*, 966−978. (b) Marcus, R. A. *Annu. Rev. Phys. Chem.* **1964**, *15*, 155−196. (c) Marcus, R. A. *Angew. Chem., Int. Ed. Engl*. **1993**, *32*, 1111−1121.

(6) (a) Sabbatini, N.; Indelli, M. T.; Gandolti, M. T.; Balzani, V. *J. Phys. Chem*. **1982**, *86*, 3585−3591. (b) Balzani, V.; Scandola, F.; Orlandi, G.; Sabbatini, N.; Indelli, M. T. *J. Am. Chem. Soc*. **1981**, *103*, 3370−3378.

(7) Shizuka, H.; Nakamura, M.; Morita, T. *J. Phys. Chem*. **1980**, *84*, 989−994.

(8) (a) Watkins, A. R. *J. Phys. Chem*. **1974**, *78*, 1885−1890. (b) Watkins, A. R. *J. Phys. Chem*. **1973**, *72*, 1207−1210

(9) (a) Mac, M.; Wirz, J.; Najbar, J. *Helv. Chim. Acta*. **1993**, *76*, 1319−1331. (b) Mac, M.; Wirz, J. *J. Chem. Phys. Lett.* **1993**, *211*, 20−26.

(10) (a) Miller, J. R.; Beitz, J. V.; Huddleston, R. K. *J. Am. Chem. Soc*. **1984**, *106*, 5057−5068. (b) Closs, G. L.; Calcaterra, L. T.; Green, N. J.; Penfield, K. W.; Miller, J. R. *J. Phys. Chem*. **1986**, *90*, 3673−3683.

(11) Ulstrup, J.; Jortner, J. *J. Chem. Phys*. **1975**, *63*, 4358−4368.

(12) Siders, P.; Marcus, R. A. *J. Am. Chem. Soc*. **1981**, *103*, 741−747.

(13) (a) Kikuchi, K.; Kokubun, H.; Koizumi, M. *Bull. Chem. Soc. Jpn*. **1968**, *41*, 1545−1551. (b) Kikuchi, K.; Watarai, H.; Koizumi, M. *Bull. Chem. Soc. Jpn*. **1973**, *46*, 749−754.

(14) Sato, C. Thesis, Tohoku University, Sendai, Japan, 1993.

(15) Mann, C.; Barnes, K. *Electrochemical Reaction in Nonaqueous Systems*; Marcel Dekker: New York, 1970.

(16) (a) Leonhardt, H.; Weller, A. *Ber. Bunsen-Ges. Phys. Chem*. **1963**, *67*, 791−795. (b) Knibbe, H.; Rehm, D.; Weller, A. *Bunsen-Ges. Phys. Chem*. **1968**, *72*, 257−263.

(17) Birks, J. B. *Photophysics of Aromatic Molecules*; Wiley: London, 1970.

(18) Sano, H.; Tachiya, M. *J. Chem. Phys*. **1979**, *71*, 1276−1282.

(19) Weller, A. *Z. Phys. Chem*. **1957**, *13*, 335−352.